

Pattern-Acquisition in Finite, Heterogenous, Delay-Coupled Swarms

Klimka Szwaykowska^{1*}, Christoffer Heckman^{1*}, Luis Mier-y-Teran-Romero^{1,2}, and Ira B. Schwartz¹

¹ U.S. Naval Research Laboratory, Code 6792, Plasma Physics Division, Nonlinear Dynamical Systems Section, Washington, DC 20375

² Bloomberg School of Public Health, Johns Hopkins University, Baltimore, MD 21205

Abstract—The self-organizing behavior of swarms of interacting particles or agents is a topic of intense research in fields extending from biology to physics and robotics. In this paper, we carry out a systematic study of how the stable spatio-temporal patterns of a swarm depend on the number of agents, in the presence of time-delayed interaction and agent heterogeneity. We show how a coherent pattern is modified as the number of agents varies, including the time required to converge to it starting from random initial conditions. We discuss the implications of our results for curve-tracking using autonomous robotic systems.

I. INTRODUCTION

The dynamics of interacting multi-agent or swarming systems in many biological, physical and engineering fields is undergoing very active research. Remarkably, these systems are able to self-organize into highly structured spatio-temporal patterns and demonstrate complex collective behaviors, with very limited information passed between individual agents. Examples in biology include bacterial colonies, schooling fish, flocking birds, swarming locusts, ants, and even pedestrians [1]–[11].

One of the practical goals in swarming research in robotics is to bring the advantages of aggregation in biological systems, such as scalability and robustness, into engineered systems. To achieve scalability, the individual agents that make up the aggregate should be simple and inexpensive, and easily added to the overall swarm. For robustness, it should be possible to have agents fail and be removed from the swarm, without significantly affecting the collective dynamics. In fact, aggregates of locally interacting agents have been proposed as a means to create scalable sensor arrays for surveillance and exploration [12]–[18]; and for the formation of reconfigurable modal systems, in which a group of simple agents can be used to accomplish a task that would be impossible for any agent individually [18]–[20].

A thorough understanding of the dynamical properties of the swarm is necessary for algorithm design and implementation. Many different approaches are possible in order to elucidate this: a number of works treat the swarm at a level of individual agents [5], [8], [9], [21]; others have attacked the problem via continuum models [4], [7], [22]. A number of studies show that even with simple interaction protocols, swarms of agents are able to converge to organized, coherent behaviors. Interestingly, environmental noise and

processing time delays affecting the agent dynamics can lead to the formation of new steady-state motions, bistability and hysteresis, or phase transitions between between co-existing steady states [23]–[25]. Noise is used to model the effects of external, unforeseen disturbances as well as unmodeled inter-agent interactions, including uncertain coupling and/or communication. On the other hand, time delays are essential for modeling finite communication and processing speeds in many interacting biological systems, including population dynamics, blood cell production, and genetic networks [26]–[28], or in mathematical models of robot networks with explicit communication and processing delays [29].

Biology has shown us that swarms exist in stable configurations composed of a great many single agents. Motivated by this observation, a number of existing works on the spatio-temporal patterns of swarm dynamics present results that are valid in the so-called “thermodynamic limit,” where the number of agents is assumed to be very large [4], [21]–[25], [30], [31]. This limiting situation is attractive on several grounds and is particularly amenable to mean-field approximations that allow one to make analytic predictions on the collective behavior of the swarm. However, in most real-world situations, the size of the swarm is limited by the cost of individual agents, bandwidth requirements, agent malfunction, etc. It is therefore important to verify how well the analytical predictions for collective motion made in the thermodynamic limit hold as swarm size is reduced.

In addition, most existing work assumes that the members of the swarm are identical. However, many practical applications involve swarms that are composed of agents with differing dynamical properties from the onset, or that become different over time due to malfunction or aging. Swarm heterogeneities lead to interesting new collective dynamics such as spontaneous segregation of the various populations within the swarm; it also has the potential to erode swarm cohesion. In biology, for example, it has been shown that sorting behavior of different cell types during the development of an organism can be achieved simply by introducing heterogeneity in inter-cell adhesion properties [32], [33]. It has also been shown that increasing the neighbor-to-neighbor attraction between cells of a single type leads to segregation of types in aggregates of self-propelled cells [34]. In robotic systems, heterogeneity may arise over time when, for example, battery depletion, or other losses of functionality, occur at different rates for different agents within the swarm. Allowing for heterogeneity in dynamical

* Co-first author

behaviors of swarm agents gives greater flexibility in system design, and is therefore desirable not only from a theoretical but also from a practical point of view.

In this work we address the issues of coherent-pattern scalability and robustness for a delay-coupled swarm with heterogeneous agents performing a path-following mission. We extend a globally delay-coupled swarm model in [23], [24] to swarms with heterogeneous agent dynamics. We conduct a careful numerical analysis to examine the scaling behavior of the coherent patterns of the swarm as the number of agents varies over a wide range. In particular, we investigate how long it takes the swarm in an arbitrary configuration to acquire a particular coherent pattern. This state exploits the segregation of heterogeneous agents in the swarm to create a state that separates agents according to their natural motion. The approach is novel in that it promotes robustness by eliminating weaker agents that might negatively affect the performance of the swarm and serve as a metric for the health of the entire swarm.

II. PROBLEM STATEMENT

We investigate the pattern-transition capabilities of a two-dimensional swarm of autonomous agents as it carries out a mission. For definitive purposes, we take this mission to be the tracking of a virtual “leader agent” that moves along an arbitrary curve \mathcal{C} . We assume that each agent can measure the distance and relative heading to all other agents in the swarm and of the virtual leader. These measurements are relatively easy to obtain using inexpensive sensors, and do not require the agents to agree on a common reference frame.

At some point during the curve-tracking, the swarm is made to transition to a stationary, ‘ring’ coherent pattern that may serve as a diagnostic state to identify the agents with degraded performance. Of particular interest is how the spatio-temporal scales of this diagnostic state depend on the number of agents present as well as the time to acquire said pattern.

We now introduce the dynamical model for the swarming agents and the virtual leader. Let $\mathbf{r}_i(t) \in \mathbb{R}^2$ denote the position of agent i in the swarm, $i \in \{1, \dots, N\}$. Each agent has self-propulsion with a preferred speed that is scaled to 1, and additionally is attracted to the other agents in the swarm and to the leader. The coupling coefficient that quantifies the attraction between agents in the swarm is a , while the coupling coefficient between each swarm agent and the leader is a_L . We consider that the attraction between agents occurs in a time-delayed fashion, on account of finite communication speeds and processing times; we assume a single, fixed time delay denoted by τ . The position of the virtual leader is given by $\mathbf{r}_L(t)$. The leader is confined to stay on the curve \mathcal{C} . Let $s \in \mathbb{R}$ denote the speed of the leader along \mathcal{C} . The dynamics of the swarm particles and leader are described by the following dimensionless

governing equations:

$$\ddot{\mathbf{r}}_i = \kappa_i \left(1 - \|\dot{\mathbf{r}}_i\|^2\right) \dot{\mathbf{r}}_i - \frac{a\kappa_i}{N} \sum_{\substack{j=1 \\ i \neq j}}^N (\mathbf{r}_i(t) - \mathbf{r}_j(t - \tau)) + a_L \kappa_i (\mathbf{r}_i(t) - \mathbf{r}_L(t)) \quad (1)$$

$$\dot{s} = (1 - s) - a_0 \|\mathbf{r}_L(t) - \mathbf{R}(t)\|, \quad (2)$$

where dots are used to denote differentiation with respect to time. The self-propulsion of agent i is modeled by the term $\left(1 - \|\dot{\mathbf{r}}_i\|^2\right) \dot{\mathbf{r}}_i$. At time t , agent i is attracted to the position of agent j at the past time $t - \tau$ and to the current position of the leader. The factor $\kappa_i \in (0, 1]$ scales the acceleration of agent i , behaving like an inverse mass. One may interpret it as a measure of the battery state of agent i or some other source of heterogeneity that impedes acceleration. We assume that for a given number of agents in the swarm, κ_i is given by a uniform distribution on $(0, 1]$. This simplified model does not include short-range repulsion or other collision-avoidance strategies; however, earlier studies with homogeneous swarms indicate that the collective dynamics of the swarm are not significantly altered by the introduction of short-range repulsion terms [23].

We will show, using simulation, that the controller described above tracks the position of the virtual leader agent along the curve. We will further show that, to achieve segregation of the swarming agents by κ , it is sufficient to set the speed of the leader agent to 0, for appropriate values of the parameters a and τ . For application of our theoretical results in a real-world setting (where number of agents is typically limited by space, cost, or communication bandwidth requirements), we run extensive numerical simulations to examine how collective behavior of the swarm depends on the number of its constituent agents N .

III. CURVE TRACKING

The goal of the curve-tracking behavior is to have the center of mass of the swarm track the length-parametrized curve \mathcal{C} . To this end, we introduce the virtual leader agent, with position $\mathbf{r}_L(t) \in \mathcal{C}$, and add a proportional control term $a_L \kappa_i (\mathbf{r}_i(t) - \mathbf{r}_L(t))$ in (1) to track the position of this agent.

The acceleration of the virtual leader along \mathcal{C} is given by (2), and includes a self-propulsion term as well as a feedback term that reduces acceleration proportionally to the distance from the virtual leader position to the swarm center of mass. A series of snapshots of the swarm tracking the virtual leader along a circular trajectory are shown in Fig. 1.

IV. DIAGNOSTIC MODE

The system is switched into diagnostic mode by setting the leader speed $s = 0$. When this happens, the swarm converges to a ring state, in which the center of mass is fixed at the position of the leader, while particles in the swarm rotate in either direction about the center, with radius that depends on the coupling constants a and a_L , and on the individual constant of acceleration κ_i .

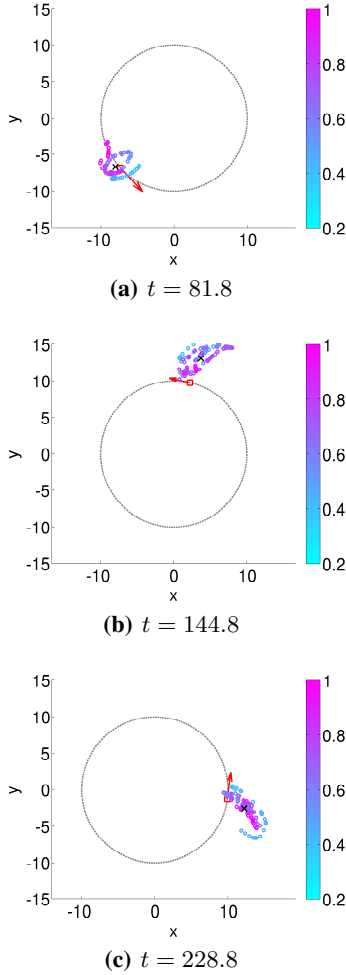


Fig. 1: Snapshots from simulation of swarm tracking a circular trajectory. The position of the virtual leader is shown by the red box; the red arrow indicates the direction of the leader agent's motion. The center of mass of the swarm is marked by a black \times . Agent positions are shown by circles, with colors indicating the respective values of κ_i . The values of κ_i in this simulation are uniformly distributed on $[0.2, 1]$. The coupling constant $a = 0.1$, $a_L = 0.06$, and the delay is $\tau = 1$. The coupling coefficient of the leader to the swarm is $a_0 = 0.06$.

In this section, we conduct a careful theoretical analysis of the center of mass dynamics of the swarm in the thermodynamic limit ($N \rightarrow \infty$), extending results presented for the leaderless, homogeneous swarm case ($a_L = 0$ and $\kappa_i = 1, \forall i \in \{1, \dots, N\}$) in [23].

Proceeding as in [23], let $\mathbf{R}(t) = \frac{1}{N} \sum_{i=1}^N \mathbf{r}_i(t)$ be the center of mass of the swarm, and let $\delta \mathbf{r}_i(t) = \mathbf{r}_i(t) - \mathbf{R}(t)$ be the position of agent i relative to the center of mass; note that $\sum_{i=1}^N \delta \mathbf{r}_i(t) = 0$. Using the change of variables

$\mathbf{r}_i(t) = \mathbf{R}(t) + \delta \mathbf{r}_i(t)$, (1) can be written as

$$\begin{aligned} \ddot{\mathbf{R}} + \delta \ddot{\mathbf{r}}_i = & \kappa_i \left(1 - \|\dot{\mathbf{R}}\|^2 - \|\delta \dot{\mathbf{r}}_i\|^2 - 2\langle \dot{\mathbf{R}}, \delta \dot{\mathbf{r}}_i \rangle \right) (\dot{\mathbf{R}} + \delta \dot{\mathbf{r}}_i) \\ & - \frac{a\kappa_i}{N} \sum_{j \neq i} (\mathbf{R}(t) + \delta \mathbf{r}_i(t) - \mathbf{R}(t - \tau) - \delta \mathbf{r}_j(t - \tau)) \\ & - a_L \kappa_i (\mathbf{R}(t) + \delta \mathbf{r}_i(t) - \mathbf{R}(t) - \delta \mathbf{r}_L(t)). \end{aligned} \quad (3)$$

Without loss of generality, we set the stationary leader position \mathbf{r}_L to 0. Following the approach in [23], we sum (3) over i , then take the limit as $N \rightarrow \infty$ and neglect all terms in $\delta \mathbf{r}$ (see [23] for a justification of this simplification). The resulting equation for the motion of the center of mass of the swarm in the thermodynamic limit is:

$$\ddot{\mathbf{R}} = \bar{\kappa} \left(1 - \|\dot{\mathbf{R}}\|^2 \right) \dot{\mathbf{R}} - (a + a_L) \bar{\kappa} \mathbf{R}(t) + a \bar{\kappa} \mathbf{R}(t - \tau), \quad (4)$$

where $\bar{\kappa} = \frac{1}{N} \sum_{i=1}^N \kappa_i$ is the mean acceleration factor. The above system has an equilibrium point at $\mathbf{R} = \dot{\mathbf{R}} = 0$, which corresponds to the ring state. As a and τ increase (for fixed values of the parameters a_L and $\bar{\kappa}$), the system undergoes a Hopf bifurcation, giving rise to a new oscillating steady-state behavior, whereby the swarm becomes more compact and organizes itself into a coherent rotating state. To ensure that the system converges to the ring state given τ and estimated $\bar{\kappa}$, we choose a and a_L so that the system lies below the first Hopf bifurcation curve (see Fig. 2).

Once the system enters the ring state, the agents with low battery power (denoted in our model by low κ_i) can be picked out from the radius of the circular trajectory they follow about the fixed center of mass. To see this, consider (3). As before, we set $\mathbf{r}_L = 0$, so that in the ring state, $\mathbf{R} = \dot{\mathbf{R}} = 0$. Equation (3) then simplifies to:

$$\begin{aligned} \delta \ddot{\mathbf{r}}_i = & \kappa_i \left(1 - \|\delta \dot{\mathbf{r}}_i\|^2 \right) \delta \dot{\mathbf{r}}_i \\ & - \frac{a\kappa_i}{N} \sum_{j \neq i} (\delta \mathbf{r}_i(t) - \delta \mathbf{r}_j(t - \tau)) - a_L \kappa_i \delta \mathbf{r}_i(t). \end{aligned} \quad (5)$$

Taking the limit as $N \rightarrow \infty$ and converting to polar coordinates (ρ_i, θ_i) , where ρ_i denotes the distance of agent i from the origin and θ_i denotes the phase, gives

$$\dot{\rho}_i = \kappa_i (1 - \rho_i^2 \dot{\theta}_i^2 - \dot{\rho}_i^2) \dot{\rho}_i + (\dot{\theta}_i^2 - (a + a_L) \kappa_i) \rho_i \quad (6)$$

$$\rho_i \ddot{\theta}_i = \kappa_i (1 - \rho_i^2 \dot{\theta}_i^2 - \dot{\rho}_i^2) \rho_i \dot{\theta}_i - 2 \dot{\rho}_i \dot{\theta}_i. \quad (7)$$

In the ring state, $\dot{\rho}_i = \ddot{\theta}_i = \dot{\theta}_i = 0$; setting these values in the above equations gives

$$\dot{\theta}_i = \pm \sqrt{(a + a_L) \kappa_i} \quad (8)$$

$$\rho_i = 1/|\dot{\theta}_i| = 1/\sqrt{(a + a_L) \kappa_i}. \quad (9)$$

Thus, in the ring state, agent i circles the stationary leader position with radius inversely proportional to κ_i . As a result, we can easily identify the agents with limited motion capabilities by distinguishing the agents whose radius in the ring state exceeds a certain pre-specified threshold. As an example, Figure 3 shows the case in which we wish to eliminate all agents with $\kappa_i \leq 0.5$; the threshold radius is then $\rho_{\text{TH}} = 1/\sqrt{0.5(a + a_L)}$ as shown in the figure.

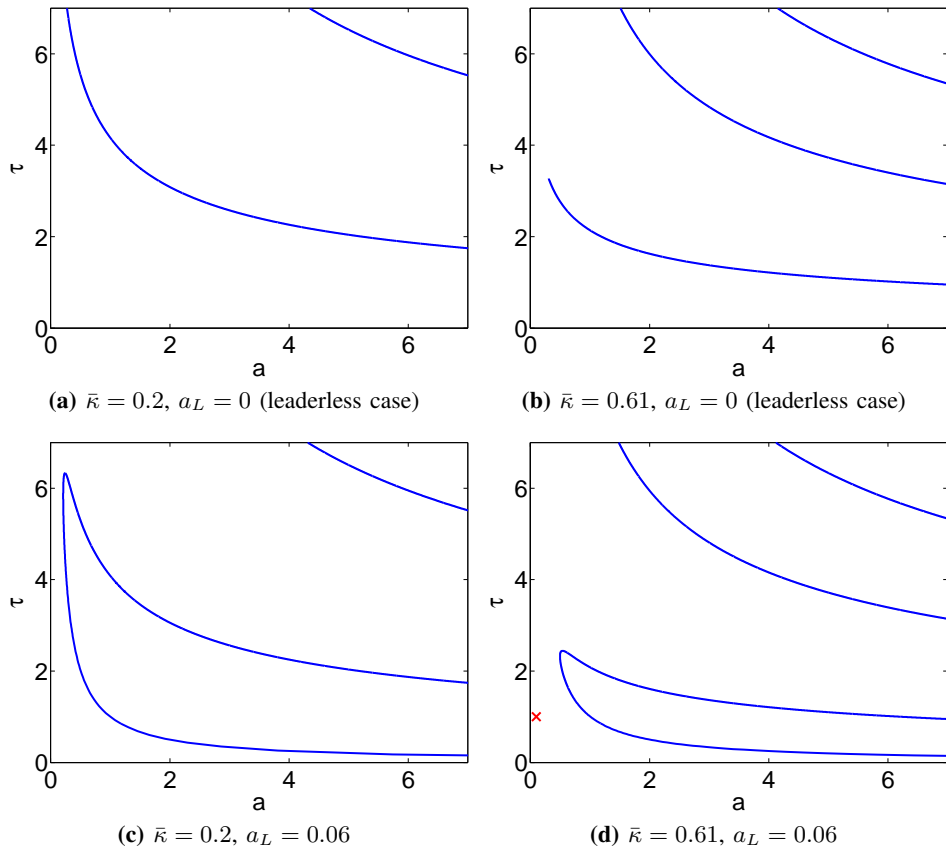


Fig. 2: The solid blue lines show τ vs a Hopf bifurcation curves for the center-of-mass heterogeneous swarm dynamics, for different values of the parameters $\bar{\kappa}$ and a_L . The simulation in Section III were run with parameter values marked by the red \times in Fig. 2d.

V. FINITE N EFFECTS

We now investigate how the spatio-temporal scales of the ring state, as well as how the length of time required to achieve it varies with the number of agents N . We consider the system to be in the ring state once the swarm’s mean radius to its center of mass has converged to a small neighborhood about the average value.

Firstly, we set $\kappa_i = 1$ for all agents and study the dependence of swarm collective motions on finite N . Using numerical simulations, we have measured the time required to converge to the ring state over 100 trials for random initial conditions at various population sizes, ranging from $N = 2$ to $N = 150$. As expected, for large N , the dynamics converge to a ‘thermodynamic limit’ and are qualitatively similar in almost all trials. Fig. 4a shows that for large population sizes the times to converge are relatively constant, but as N decreases the convergence time and the variance of these times increases dramatically. For very small N the system is far less predictable and will at times converge to a periodic motion different from the ring state.

When agents do converge to the ring state, we can make the following theoretical prediction for the radius ρ of the ring in the finite- N case, under the assumption that agents are uniformly distributed along the ring:

$$\omega^2 = a \left(1 - \frac{1}{2}(1 - \cos \omega\tau) \right), \quad (10)$$

$$\rho = \frac{1}{\omega} \sqrt{1 + \frac{a \sin \omega\tau}{N\omega}}. \quad (11)$$

where ω is the angular frequency of the agents moving about the ring. For $N \rightarrow \infty$ these reduce to $\omega^2 = a$ and $\rho = \frac{1}{\omega}$, which agrees with Eq. (9) for the ring radius in the large N limit, remembering that $a_L = 0$ and $\kappa_i = 1$ in the current situation. In this case of homogeneous κ , Figure 5 shows good agreement between the simulated radius and velocity and the predictions of these quantities as given above.

For the uniform κ case, When N is very small (less than 10), a wealth of behavior emerges that is far less likely for large N . For example, when $N = 5$ the most prevalent state arranged all five agents equally along a circle in a pentagonal pattern, rotating in the same direction. These symmetric patterns exhibit extremely rapid convergence times from random initial conditions, which explains the surprising rapid decrease in convergence times for small N shown in Fig. 4a. Formally identifying these patterns and justifying their unique behavior is an area of future work that we plan to investigate.

Next we consider the case of distributed κ_i as described in Section II. We repeat the numerical simulations conducted

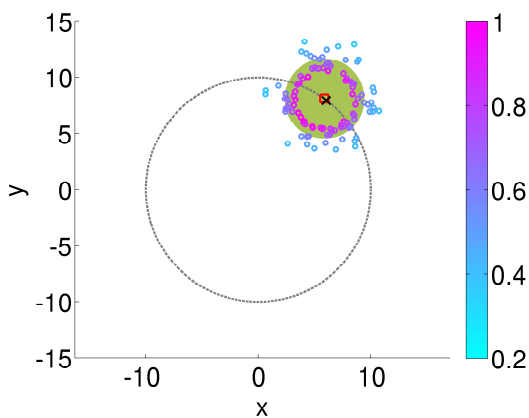


Fig. 3: Snapshot from simulation of swarm in diagnostic state. The virtual leader is marked by the red box; the center of mass of the swarm is marked by a black \times and is coincident with the leader position. Agent positions are shown by circles, with colors indicating the respective values of κ_i . All agents with $\kappa_i > 0.5$ are contained inside the green circle; agents which lie outside may be eliminated.

for $\kappa_i = 1$ to measure the time required to converge to an apparent ring state over 100 trials with randomly distributed initial conditions and κ_i uniformly distributed over $[0.2, 1]$ in each trial over various values of N . The results of these simulations are shown in Figure 4b, demonstrating a similar relationship of time-to-convergence with N as in the uniform κ case. The mean radius of the ring converges to approximately 1.4, which is consistent with the mean-field prediction for $a = 1$, $a_L = 0$, and κ_i uniformly distributed on $[0.2, 1]$. Fig. 6 shows the mean ring radius and velocity of agents in the ring state.

VI. CONCLUSION

In this paper we have used curve following as a sample application for the use of collectively moving autonomous agents. We have shown how the naturally-emerging collective motions of interacting autonomous agents can be exploited to segregate agents with different dynamical properties, even when they follow the same overall behaviors as other agents in the swarm (in our case, we separated out agents with lower acceleration factors, corresponding to depleted battery state or mechanical failure).

Furthermore, we have analyzed collective motions of delay-coupled heterogeneous agents. We tested the limits of the commonly-used thermodynamic limit for modeling swarm populations by considering the effects of finite swarm size on time to converge to a given pattern (in this case, the ring state), and by comparing the ring state radius and circulating velocity with theoretical predictions based on the thermodynamic model. We have verified that the theoretical predictions of the thermodynamic limit hold very well for large (100+ agents) and medium (20+ agents) swarms, but break down for smaller numbers of agents. In this few-agent limit, the swarm often does not converge to the expected

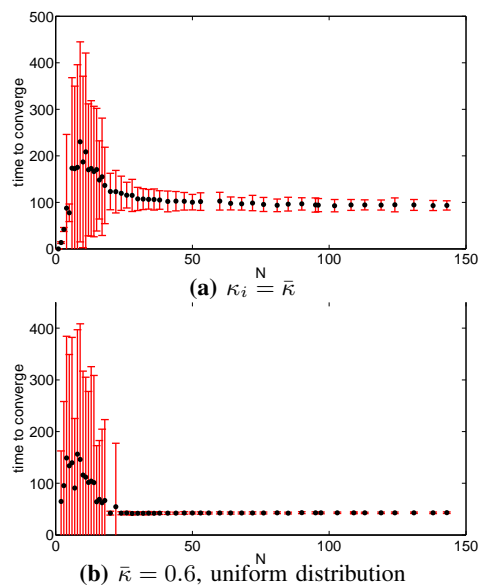


Fig. 4: Time for the system to converge to ring state for different values of swarm size N . Parameter values are $a = 1$, $a_L = 0$, $\tau = 1$ and $\kappa_i = 1$ for all i (top panel) and κ_i uniformly distributed on $[0.2, 1]$ (bottom panel).

ring, and we observe the emergence of more exotic collective periodic patterns.

In the current work, we have assumed that the agents in the swarm are globally coupled. This is generally not feasible in swarms of more than a few agents, on account of communication bandwidth requirements. In future work, we will relax this assumption to consider less than fully connected swarms. We will also consider the effects of inter-agent repulsion on the collective dynamics.

Our work represents an important link between theory of aggregate systems (generally developed in the thermodynamic limit) and practical applications of swarming systems (which generally contain few agents).

ACKNOWLEDGMENTS

This research was performed while KS and CRH held a National Research Council Research Associateship Award at the U.S. Naval Research Laboratory. LMTR is a post doctoral fellow at Johns Hopkins University supported by the National Institutes of Health. This research is funded by the Office of Naval Research contract no. N0001412WX2003 and the Naval Research Laboratory 6.1 program contract no. N0001412WX30002.

REFERENCES

- [1] E. O. Budrene and H. C. Berg, “Dynamics of formation of symmetrical patterns by chemotactic bacteria,” *Nature*, vol. 376, pp. 49–53, 1995.
- [2] J. Toner and Y. Tu, “Long-range order in a two-dimensional dynamical xy model: How birds fly together,” *Phys. Rev. Lett.*, vol. 75, no. 23, pp. 4326–4329, 1995.
- [3] J. K. Parrish, “Complexity, pattern, and evolutionary trade-offs in animal aggregation,” *Science*, vol. 284, pp. 99–101, Apr 1999.
- [4] C. M. Topaz and A. L. Bertozzi, “Swarming Patterns in a Two-Dimensional Kinematic Model for Biological Groups,” *SIAM Journal on Applied Mathematics*, vol. 65, pp. 152–174, Jan. 2004.

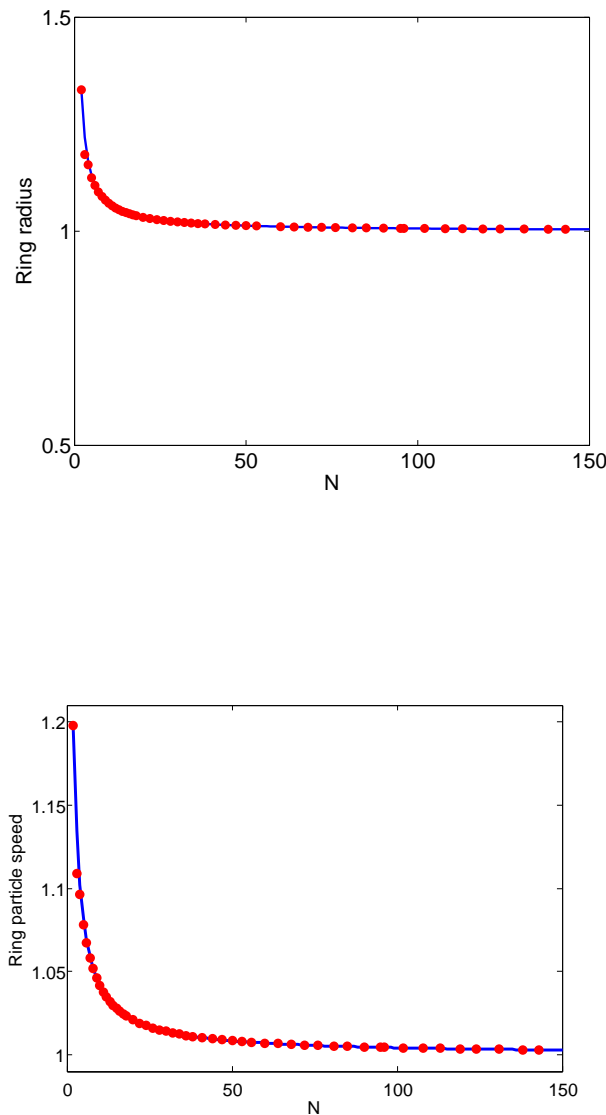


Fig. 5: Radius and average speed of agents in the ring state for different values of swarm size N . Red dots indicate numerical simulations and the blue lines are predicted by theory. Parameter values: $a = 1$, $a_L = 0$, $\tau = 1$, and $\kappa_i = 1$ for all i .

- [5] D. Helbing and P. Molnar, “Social force model for pedestrian dynamics,” *Physical Review E*, vol. 51, no. 5, pp. 4282–4286, 1995.
- [6] F. D. C. Farrell, M. C. Marchetti, D. Marenduzzo, and J. Tailleur, “Pattern formation in self-propelled particles with density-dependent motility,” *Phys. Rev. Lett.*, vol. 108, p. 248101, Jun 2012.
- [7] A. A. Polezhaev, R. A. Pashkov, A. I. Lobanov, and I. B. Petrov, “Spatial patterns formed by chemotactic bacteria *Escherichia coli*,” *The International journal of developmental biology*, vol. 50, pp. 309–314, Jan. 2006.
- [8] K. Tunström, Y. Katz, C. C. Ioannou, C. Huepe, M. J. Lutz, and I. D. Couzin, “Collective states, multistability and transitional behavior in schooling fish,” *PLoS computational biology*, vol. 9, p. e1002915, Jan. 2013.

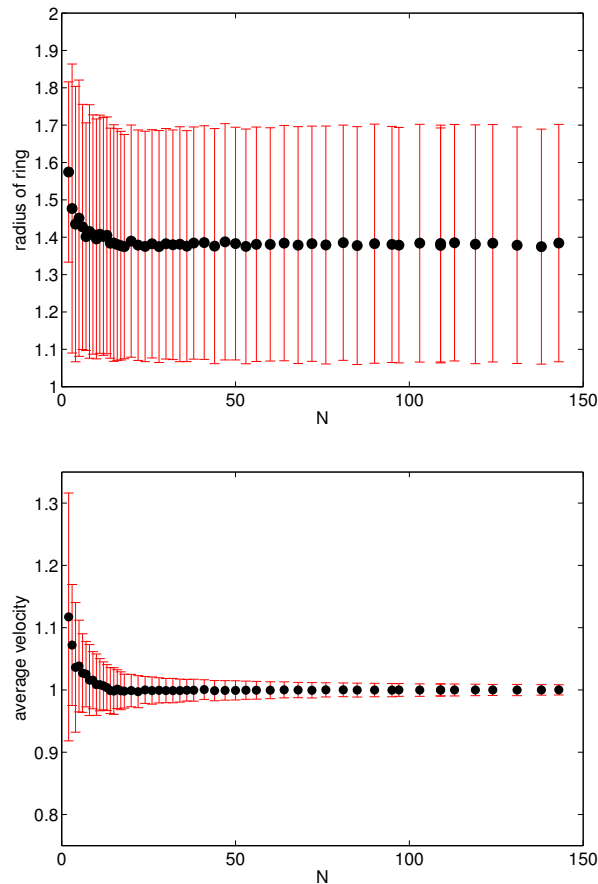


Fig. 6: Radius and average speed of agents in the ring state for different values of swarm size N with uniformly distributed values of κ . Parameter values: $a = 1$, $a_L = 0$, $\tau = 1$, and κ_i uniformly distributed on $[0.2, 1]$.

- [9] S.-H. Lee, “Predator’s attack-induced phase-like transition in prey flock,” *Physics Letters A*, vol. 357, pp. 270–274, Sept. 2006.
- [10] S. Mishra, K. Tunström, I. D. Couzin, and C. Huepe, “Collective dynamics of self-propelled particles with variable speed,” *Phys. Rev. E*, vol. 86, p. 011901, Jul 2012.
- [11] C. Xue, E. O. Budrene, and H. G. Othmer, “Radial and spiral stream formation in *Proteus mirabilis* colonies,” *PLoS Comput Biol*, vol. 7, p. e1002332, 12 2011.
- [12] P. Bhatta, E. Fiorelli, F. Lekien, N. E. Leonard, D. A. Paley, F. Zhang, R. Bachmayer, D. M. Fratantoni, R. E. Davis, and R. J. Sepulchre, “Coordination of an underwater glider fleet for adaptive sampling,” in *Proceedings of the International Workshop on Underwater Robotics*, no. August, pp. 61–69, 2005.
- [13] W. Wu and F. Zhang, “Cooperative exploration of level surfaces of three dimensional scalar fields,” *Automatica*, vol. 47, pp. 2044–2051, Sept. 2011.
- [14] N. Leonard and E. Fiorelli, “Virtual leaders, artificial potentials and coordinated control of groups,” in *Proc. of the 40th IEEE Conference on Decision and Control.*, vol. 3, pp. 2968–2973, 2002.
- [15] E. Justh and P. Krishnaprasad, “Steering laws and continuum models for planar formations,” in *Proc. of the 42nd IEEE Conference on Decision and Control.*, vol. 4, pp. 3609–3614, 2004.
- [16] D. Morgan and I. B. Schwartz, “Dynamic coordinated control laws in multiple agent models,” *Phys. Lett. A*, vol. 340, no. 1-4, pp. 121–131, 2005.
- [17] Y. Chuang, M. R. D’Orsogna, D. Marthaler, A. L. Bertozzi, and L. S. Chayes, “State transitions and the continuum limit for a 2D interacting, self-propelled particle system,” *Physica D: Nonlinear Phenomena*, vol. 232, pp. 33–47, Aug. 2007.
- [18] K. M. Lynch, I. B. Schwartz, P. Yang, and R. A. Freeman, “Decen-

- tralized Environmental Modeling by Mobile Sensor Networks,” IEEE Transactions on Robotics, vol. 24, pp. 710–724, June 2008.
- [19] S. Kar and J. M. F. Moura, “Distributed linear parameter estimation in sensor networks: Convergence properties,” Oct. 2008.
- [20] M. Dorigo, D. Floreano, L. M. Gambardella, F. Mondada, S. Nolfi, T. Baaboura, M. Birattari, M. Bonani, M. Brambilla, A. Brutschy, D. Burnier, A. Campo, A. L. Christensen, A. Decugniere, G. Di Caro, F. Ducatelle, E. Ferrante, A. Forster, J. M. Gonzales, J. Guzzi, V. Longchamp, S. Magnenat, N. Mathews, M. Montes de Oca, R. O’Grady, C. Pinciroli, G. Pini, P. Retornaz, J. Roberts, V. Sperati, T. Stirling, A. Stranieri, T. Stutzle, V. Trianni, E. Tuci, A. E. Turgut, and F. Vaussard, “Swarmanoid: A Novel Concept for the Study of Heterogeneous Robotic Swarms,” IEEE Robotics & Automation Magazine, vol. 20, pp. 60–71, Dec. 2013.
- [21] T. Vicsek, A. Czirok, E. Ben-Jacob, I. Cohen, and O. Shochet, “Novel type of phase transition in a system of self-driven particles,” 2006.
- [22] L. Edelstein-Keshet, D. Grunbaum, and J. Watmough, “Do travelling band solutions describe cohesive swarms? An investigation for migratory locusts,” Journal of Mathematical Biology, vol. 36, pp. 515–549, July 1998.
- [23] L. Mier-y-Teran Romero, E. Forgoston, and I. B. Schwartz, “Coherent Pattern Prediction in Swarms of Delay-Coupled Agents,” IEEE Transactions on Robotics, vol. 28, pp. 1034–1044, Oct. 2012.
- [24] L. Mier-y-Teran Romero, E. Forgoston, and I. B. Schwartz, “Noise, Bifurcations, and Modeling of Interacting Particle Systems,” in Proceedings of the IEEE/RSJ International Conference on Intelligent Robots and Systems, pp. 3905–3910, Jan. 2011.
- [25] L. Mier-y Teran and I. B. Schwartz, “Capturing pattern bi-stability dynamics in delay-coupled swarms,” Euro. Phys. Lett., vol. 105, no. 2, p. 20002, 2014.
- [26] A. Martin and S. Ruan, “Predator-prey models with delay and prey harvesting,” Journal of Mathematical Biology, vol. 43, pp. 247–267, Sept. 2001.
- [27] S. Bernard, J. Bélair, and M. C. Mackey, “Bifurcations in a white-blood-cell production model,” Comptes Rendus Biologies, vol. 327, pp. 201–210, Mar. 2004.
- [28] N. A. M. Monk, “Oscillatory Expression of Hes1, p53, and NF- κ B Driven by Transcriptional Time Delays,” Current Biology, vol. 13, pp. 1409–1413, 2003.
- [29] E. Forgoston and I. B. Schwartz, “Delay-induced instabilities in self-propelling swarms,” Physical Review E, vol. 77, no. 302, p. 035203, 2008.
- [30] A. J. Leverenz, C. M. Topaz, and A. J. Bernoff, “Asymptotic Dynamics of Attractive-Repulsive Swarms,” SIAM Journal on Applied Dynamical Systems, vol. 8, pp. 880–908, Jan. 2009.
- [31] M. Burger, J. Haškovec, and M.-T. Wolfram, “Individual based and mean-field modeling of direct aggregation,” Physica D. Nonlinear phenomena, vol. 260, pp. 145–158, Oct. 2013.
- [32] M. S. Steinberg, “Reconstruction of Tissues by Dissociated Cells,” Science, vol. 141, pp. 401–408, Aug. 1963.
- [33] F. Graner, “Simulation of the differential adhesion driven rearrangement of biological cells,” Physical Review E, vol. 47, no. 3, pp. 2128–2154, 1993.
- [34] J. Belmonte, G. Thomas, L. Brunnet, R. de Almeida, and H. Chaté, “Self-Propelled Particle Model for Cell-Sorting Phenomena,” Physical Review Letters, vol. 100, p. 248702, June 2008.